University of South Florida
DIGITAL COMMONS
@ UNIVERSITY OF SOUTH FLORIDA
Digital Commons @ University of South Florida

Internal Medicine Faculty Publications
Internal Medicine

3-6-2018

Splenic Leukocytes Define the Resolution of Inflammation in Heart Failure

Ganesh V. Halade
ghalade@usf.edu

Paul C. Norris
Brigham and Women's Hospital

Vasundhara Kain
The University of Alabama at Birmingham

Charles N. Serhan
Brigham and Women's Hospital

Kevin A. Ingle
The University of Alabama at Birmingham

Follow this and additional works at: https://digitalcommons.usf.edu/intmed_facpub

Scholar Commons Citation

Halade, Ganesh V.; Norris, Paul C.; Kain, Vasundhara; Serhan, Charles N.; and Ingle, Kevin A., "Splenic Leukocytes Define the Resolution of Inflammation in Heart Failure" (2018). *Internal Medicine Faculty Publications*. 26.
https://digitalcommons.usf.edu/intmed_facpub/26

This Article is brought to you for free and open access by the Internal Medicine at Digital Commons @ University of South Florida. It has been accepted for inclusion in Internal Medicine Faculty Publications by an authorized administrator of Digital Commons @ University of South Florida. For more information, please contact digitalcommons@usf.edu.

Author Manuscript

Author Manuscript

Author Manuscript

Author Manuscript

HHS Public Access

Author manuscript

Sci Signal. Author manuscript; available in PMC 2018 September 19.

Published in final edited form as:

Sci Signal. ; 11(520): . doi:10.1126/scisignal.aao1818.

Splenic leukocytes define the resolution of inflammation in heart failure

Ganesh V. Halade[1], **Paul C. Norris**[2], **Vasundhara Kain**[1], **Charles N. Serhan**[2], and **Kevin A. Ingle**[1]

[1]Division of Cardiovascular Disease, Department of Medicine, The University of Alabama at Birmingham, Alabama, 35294;

[2]Center for Experimental Therapeutics and Reperfusion Injury, Department of Anesthesiology, Perioperative and Pain Medicine, Brigham and Women's Hospital, Boston, Massachusetts, 02115 United States

Abstract

Inflammation promotes healing in myocardial infarction but if unresolved, it leads to heart failure. To define the inflammatory and resolving responses, we quantified leukocyte trafficking and specialized proresolving mediators (SPMs) in the infarcted left ventricle and spleen after myocardial infarction, with the goal of distinguishing inflammation from its resolution. Our data suggest that the spleen not only served as a leukocyte reservoir but also was the site where SPMs were actively generated after coronary ligation in mice. Before myocardial infarction, SPMs were more abundant in the spleen than in the left ventricle. At day 1 after coronary ligation, the spleen was depleted of leukocytes, a phenomenon that was associated with greater numbers of leukocytes in the infarcted left ventricle and increased generation of SPMs at the same site, particularly resolvins, maresin, lipoxins, and protectin. In addition, the infarcted left ventricle showed increased expression of genes encoding lipoxygenases and enhanced production of SPMs generated by these enzymes. We found that macrophages were necessary for SPM generation. The abundance of SPMs in the spleen before myocardial infarction and increased SPM concentrations in the infarcted left ventricle within 24 hours after myocardial infarction were temporally correlated with the resolution of inflammation. Thus, the acute inflammatory response coincided with the active resolving phase in post-myocardial infarction and suggests that further investigation into macrophage-derived SPMs in heart failure is warranted.

One-sentence summary:

Correspondence author: Ganesh V. Halade, Ph.D., Department of Medicine, Division of Cardiovascular Disease, The University of Alabama at Birmingham, 703 19th Street South, MC 7755, Birmingham, AL 35294, (phone) 205-996-4139, (fax) 205-975-5150, ganeshhalade@uabmc.edu.

Author contributions: G.V.H. and K.A.I performed myocardial infarction surgery and echocardiography analysis. P.C.N. and C.N.S. performed LC-MS/MS lipidomics and contributed to manuscript and LC-MS-MS figure preparation. V.K. performed flow cytometry, measured gene expression and contributed to manuscript and figure preparation. G.V.H. designed, performed and executed the experiments and contributed to the manuscript and figure preparations.

Competing interests: The authors declare that they have no competing interests.

Data and materials availability: All data needed to evaluate the conclusions in the paper are present in the paper or the Supplementary Materials.

Author Manuscript Author Manuscript Author Manuscript Author Manuscript

Leukocytes mobilize to the heart and may be the source of inflammation-resolving lipids after myocardial infarction.

Leukocytes mobilize from the spleen to the ischemic heart and generate inflammation-resolving lipids after myocardial infarction.

Editor's summary: Calming the heart after a heart attack

Although leukocytes can trigger inflammation that aggravates a heart attack, they can also produce bioactive resolving mediators that suppress inflammation. Halade *et al.* tracked leukocyte populations and measured the concentrations of pro-resolving bioactive mediators that attenuate inflammation in mice subjected to coronary ligation, an experimental method of inducing myocardial infarction that progresses to irreversible heart failure. Their analysis suggests that leukocytes were mobilized from the spleen to the infarcted heart to produce pro-resolving mediators and specific depletion of macrophages was associated with the lack of pro-resolving mediators biosynthesis. Thus, generally preventing immune cell infiltration after a heart attack may also delay healing and recovery by allowing inflammation to continue abated.

Introduction

Chronic and non-resolving inflammation is a prominent factor in cardiovascular diseases, particularly in heart failure (HF) pathology following myocardial infarction (MI) (1–3). After MI, self-healing occurs in mice but not in humans. Mammals respond to an acute injury by trafficking leukocytes to the injury site, which generate eicosanoids such as prostaglandins (PGs) and leukotrienes (LTs) from essential and conditional fatty acids and many cytokines and chemokines (4, 5). To control MI-mediated inflammation or infection-induced myocarditis, diverse leukocytes (neutrophils, monocytes/macrophages) have a major role in resolving inflammation; however, the role of leukocytes in resolving phase still remains unclear in myocardial healing. Given the excessive inflammation in chronic HF patients, it is critical to understand the sequential healing mechanism(s) in mice to identify new targets to delay pathological left ventricle (LV) remodeling in HF.

Traditionally, post-MI healing and outcome is divided into three phases. The initiation phase encompasses the initial minutes to hours or few days of the acute inflammatory phase. The resolution phase lasts a few days to weeks and encompasses the reparative or resolving phase. Finally, the progression phases lasts weeks to months or years depending on the resolution phase, which if defective, leads to LV dysfunction, chronic HF, morbidity and mortality (6). Current research focuses on the acute inflammatory response, with the notion that the presence of neutrophils or a differential subset of monocyte/macrophages are the hallmark of inflammation and that therefore controlling inflamed leukocytes will offer cardioprotection (7). However, multiple approaches in >20,000 papers have shown ways to reduce infarct size but these results have rarely been translated to therapeutic products (8). Therefore, we sought to quantify the acute and resolving response in a temporal-spatial manner post-MI.

In the post-MI initiation phase, ~50% of leukocytes travel from the splenic reservoir through the circulation to the site of LV injury that generates edematous inflammatory milieu but

Author Manuscript Author Manuscript Author Manuscript Author Manuscript

these leukocytes have not been chemically quantitated to decode their phenotype (9). We hypothesized that splenic leukocytes actively participated in LV healing and govern the resolution of inflammation through generating specialized proresolving mediators (SPMs) (Figure 1A). SPMs are bioactive lipid mediators that include lipoxins, resolvins, protectins and maresins and are enzymatically produced during the resolution of inflammation (10). Neutrophils and monocyte/macrophages populate the infarcted area that shows LV dysfunction (fractional shortening <15%) post-MI. Here, we determined the temporal dynamics of inflammation and resolution in the acute and resolving phases in the LV and spleen post-MI. Thus, the present report suggests that splenic leukocytes, particularly macrophages, promote LV healing by generating SPMs and mobilizing precursor fatty acid substrates. These results show that leukocyte turnover is essential for acute LV healing by amplifying the generation of SPMs at the site of injury that help to resolve inflammation.

Although lipid metabolizing enzymes such as lipoxygenase (LOX) and cyclooxygenase (COX) have been investigated for the their ability to resolve inflammation post-MI (11), COX-2 inhibition results in more MI events for patients (12). Therefore, we attempted to determine the temporal role(s) of LOXs and COXs in SPM appearance for LV healing post-MI. LOXs generated bioactive(s) in the LV, while COXs generated prostanoids in the spleen to promote successful resolution of inflammation. Thus, these results demonstrate that during post-MI healing, the essential innate acute response coincides with the resolving phase during which LOX-mediated SPMs are generated in the infarcted LV in HF pathology.

Results

LOX expression increases in the infarcted LV to generate SPMs post-MI.

In mice subjected to permanent coronary ligation (Fig. 1A), the spleen displayed decreased weight (Table 1), potentially because of splenic leukocyte mobilization to the infarcted area. Further, the LV displayed a significant weight increase due to the edema that is characteristic of MI, stroke and other ischemic injury (Table 1). We evaluated naïve control mice and post-MI at day 1 (d1) and day 5 (d5) for LV geometry, fractional shortening and infarct area. Long axis B-mode with speckle tracking analyses showed reduced fractional shortening, strain and strain rate recapitulates post-MI structural HF pathology (Fig. 1B–D). The histology of LV mid-cavity sections indicated progressive dilation, wall thinning and signs of acute HF pathology in post-MI mice at d1 and d5 (Fig. 1E–F). Thus, MI-induced LV remodeling was marked with dilation-induced changes in LV size, function and geometry with splenic leukocyte depletion and marked edematous milieu in the LV and lung post-MI (Table 1 and Fig. S1, A to D). Gene expression analysis showed that genes encoding LOXs involved in initiating SPM production showed higher levels in the infarcted LV compared to those in the spleen (Fig. 1G–I). *ALOX15* peaked in the LV infarcted area within 24 hours post-MI and returned to naïve control levels by d5 post-MI (Fig. 1G), while *ALOX5* and *ALOX12* showed sustained increases in expression in the infarcted LV and spleen at d1 to d5 post-MI compared to d0 naïve controls (Fig. 1H–I). *COX-1* (which is constitutively expressed) and *COX-2* (which is inducibly expressed) were significantly higher in the spleen than the LV both pre- and post-MI. *COX-1* showed increased expression in spleen post-MI but decreased expression in infarcted LV at d1 post-MI. Post-MI *COX-2* expression was

Author Manuscript Author Manuscript Author Manuscript Author Manuscript

increased in spleen and LV within 24 hours which was sustained until d5 (Fig. 1J–K). Thus, MI-induced, organ-specific differential expression of genes encoding LOXs and COXs in the acute response may lead to diversified docosanoid and prostanoid production in the LV post-MI.

Increased LOX expression is associated with D-series SPM production in the infarcted LV post-MI

Because the expression of LOX- and COX-encoding genes were differentially increased in the infarcted LV and post-MI spleens, we measured the LOX and COX-derived SPM resolution metabolome in the LV to confirm increased activity. In response to MI at d1, SPMs in the infarcted LV were increased ~4.5 fold compared to no-MI naïve controls (Fig. 2A) while the spleen SPMs were decreased ~1.4 fold compared to naïve control at d1 post-MI. By day 5 post-MI, SPMs in the infarcted LV were further increased, suggesting continuous resolution, and the spleen returned to baseline SPM levels comparable to those in naïve controls (Fig. 2B). In the initiation phase of MI, with acute leukocyte infiltration in the infarcted LV, the DHA metabolome amplified and peaked with significant increases in resolvins, protectin and mareisn (RvD1, RvD3, RvD4, RvD5, RvD6, AT-RvD1, PD1, MaR1, 7S,14S-diHDHA and 4S,14S-diHDHA) compared to naïve controls and d5 post-MI that were each identified using LC-MS-MS (Table S1, Fig. S2 A–B and Fig. S3 A–B). Likewise, single E-series resolvin (RvE2) was increased from eicosapentaenoic acid (EPA) metabolome at d1 post-MI compared to no-MI (Table S1, Fig. S2 A–B and Fig. S3 A–B). In the arachidonic acid (AA) metabolome, the infarcted LV showed significant increases in the lipoxins and prostaglandins (LXB_4, AT-LXA_4, 5S,15S-diHETE, 5S,12S-diHETE and $PGF_{2\alpha}$) compared to no-MI and d5 post-MI (Table S1, Fig. S2 A–B and Fig. S3 A–B). From initiation to termination of the acute phase, LXA_4, PGD_2, TXB_2 and AT-PD1 were showed sustained increase in response to MI compared to no-MI naïve controls. Thus, splenic leukocyte trafficking to the infarcted LV coincides with the peak of temporal D-series resolution metabolome post-MI.

Splenic leukocytes activated Class Switching SPM generation in spleen and infarcted LV post-MI

The spleen serves as an active site for extramedullary monocytopoiesis post-MI in mice (13). In the clinical setting, spleen metabolic activity defines the future HF risk (14); therefore, we determined the splenic SPM resolution metabolome (D- and E-series resolvins, maresin, protectin and lipoxins) pre and post-MI. (Fig. 2A–B). We found that the spleen not only supplied leukocytes post-MI but was also the site of SPM biosynthesis. These SPMs included RvD1, RvD4, LXB_4, and the prostaglandins PGD_2, PGE_2 and $PGF_{2\alpha}$ (Table S2). Of note, naïve spleen contained higher levels of leukocyte class-switching SPMs such as RvD5, RvD6, PD1, AT-PD1, MaR1, LXA_4, AT-LXA_4, AT-LXB_4 compared to naïve LV (~ <10 pg/50 mg LV tissue) (Fig. 2A). We also measured the fatty acids from which SPMs are generated. Post-MI extramedullary monocytopoiesis in spleen was accompanied by mobilization and increased amounts of the fatty acids (AA; arachidonic acid, DHA; docosahexaenoic acid and EPA; eicosapentaenoic acid) at d1 post-MI (Tables S1 and S2; Fig. 2A and 2B). To understand whether resolution metabolome kinetics ran parallel with leukocyte kinetics, we next performed detailed temporal analysis of cellular infiltration in

Author Manuscript Author Manuscript Author Manuscript Author Manuscript

the post-MI LV and spleen at d1 and d5 post-MI. The total number of infiltrating $CD45^+$/$CD11b^+$ leukocytes gradually increased after MI from d1 to d5. Infarcted LV had more $CD45^+$/$CD11b^+$ leukocytes at d1 (4 fold) and at d5 (9 fold) compared to spleen post-MI (Fig. S4 A–B). Furthermore, the $F4/80^+$ population was increased in both LV and spleen, with a greater accumulation of $F4/80^+$ cells at d5 post-MI in infarcted LV compared to spleen (Fig. 3A and 3B). The MI-induced leukocyte-derived chemoattractant LTB_4 promotes adhesion and infiltration of neutrophils but lipoxins (LXA_4 and LXB_4) also regulate leukocyte infiltration and clearance to turn on resolving responses. Naïve spleen showed higher levels of LTB_4 which decreased with time by d5 post-MI. Leukocytes were mobilized from spleen to infarcted LV, as suggested by the presence of higher levels of LTB_4-induced inflammation and lower levels of LTB_4 in spleen from d1-d5 post-MI (Fig. 3C). In contrast, LXB_4 and AT-LXA_4 spiked at d1 post-MI, particularly in the spleen (Fig. 3D–E). Consistent with neutrophils ($Ly6G^+$) being the first responders, they were activated and infiltrated the infarcted LV, peaking at d1 post-MI both in LV and spleen; notably, the percentage of $Ly6G^+$ cells significantly dropped from d1 to d5 post-MI in LV and spleen (Fig. 4A–B). Neutrophil recruitment peaked within 24 h, which coincided with the increase in RvD1 in spleen and RvD1 and RvD5 in infarcted LV. These results suggested that D-series Rvs are produced in a site specific manner (Fig. 4C–D). Numerically, macrophages were the predominant cells in the infarcted LV and peaked at d5 post-MI. The macrophages showed a biphasic pattern of activation on the basis of Ly6C expression (Fig. 5A). M1 ($Ly6C^{high}$; Fig. 5B) macrophages dominated d1 post-MI, whereas M2 ($Ly6C^{low}$; Fig. 5C) macrophages increased more gradually and peaked at d5 post-MI in LV. Maresin 1 (MaR1; macrophage mediators in resolving inflammation) levels were relatively higher in spleen before MI; after leukocyte mobilization, MaR1 was lowered in spleen but spiked in the infarcted LV post-MI, suggesting that the spleen not only acts as a source of SPMs but may supplied the cells that produce SPMs at the site of injury (Fig. 5D). Thus, the leukocytes are activated simultaneously in the spleen and infarcted LV post-MI; however, SPM biosynthesis is higher in the infarcted LV compared to spleen post-MI.

Splenic leukocytes expand in the infarcted LV and acquire resolving phenotypes post-MI

Next, we assessed the pro-inflammatory and alternatively activated subset of neutrophils and macrophages in the infarcted LV and post-MI spleen. At d5 post-MI, the LV had more $Ly6G^+$/$CD206^+$ (N2) neutrophils compared with spleen (Fig. 6A–B). CD206 expression indicates resolving phenotypic variability of neutrophils and macrophages. We observed higher number of $CD206^+$ neutrophils at d1 and d5 post-MI in infarcted LV compared with spleen (Fig. 6A and B). Splenic leukocyte recruitment and regulation of innate inflammatory cells is necessary to prevent non-resolving inflammation and to achieve controlled repair (3, 9). We validated that infarcted LV and post-MI spleens contained a higher percentage of $CD11b^+F4/80^+$ macrophages compared to the naive control which displayed a biphasic pattern on the basis of CD206 expression. At d1 post-MI d1, $Ly6G^-$/$CD206^+$ (Fig. 6C), $Ly6G^+$/$CD206^+$ (Fig. 6D), $Ly6C^{high}CD206^+$ (Fig. 6E) macrophages were significantly increased in the infarcted LV, suggesting that alternatively activated macrophages and neutrophils were increased within 24 h. Resolving macrophages ($Ly6C^{low}CD206^+$) began to increase at d1 and peaked at d5 post-MI in the LV compared to spleen and no-MI control (Fig. 6F). Thus, splenic leukocytes were primarily expanded to resolving phenotypes in the infarcted LV,

Author Manuscript Author Manuscript Author Manuscript Author Manuscript

suggesting progression towards resolution of inflammation post-MI. However, neutrophil and macrophage variability extends beyond classifications of pro-inflammatory M1 or N1 and resolving M2 or N2 phenotypes which depend on the generation of class switching SPMs in the infarcted LV and spleen post-MI (15).

Depletion of macrophages reduces *LOX* expression and SPM generation post-MI

Since macrophages are centrally involved in myocardial healing in mice and depletion of macrophages magnifies post-MI mortality, we assessed the macrophage-derived lipid mediator secretome after injecting mice with clodronate (CLD) liposomes to deplete macrophages (Fig. 7A). Flow cytometry data indicated that CLD-injected mice had a ~2.5 fold decrease in monocytes ($CD11b^+/CD45^+$) and macrophages ($CD11b^+/F4/80^+$) in spleen and a ~1.4 fold decrease in the infarcted LV within 24 h compared to MI-control, confirming post-MI leukocyte depletion (Fig. 7B–E). In response to CLD-mediated depletion, *ALOX15* (Fig. 7F), *ALOX12* (Fig. 7G), and *ALOX5* (Fig. 7H) mRNA expression were decreased while *COX-2* (Fig. 7I) and *COX-1* (Fig. 7J) mRNA expression were increased in the infarcted LV compared to MI-control. To validate the post-MI activity of LOXs and COXs in spleen and infarcted LV, we used targeted metabolipidomics that emphasized SPMs. Only 3 SPMs (LXA_4, AT-LXA_4 and RvD4) were detected in the infarcted LV and spleen of CLD-injected mice (Fig. 7K, 7L, and 7M) compared to infarcted LV of MI control mice which displayed high concentrations of SPMs (D- and E-series resolvins, protectins, maresin and lipoxins) (Tables S1 and S2). Further, CLD-injected, post-MI infarcted LV and spleen showed decreased levels of LTB_4 (Fig. 7N), LXB_4 (Fig. 7O), and PGE_2 (Fig. 7P) compared to MI-control (Tables S1 and S2, Fig. S5 A–B). These results showed that the macrophage secretome contributed most of the SPMs during acute healing of the LV.

Resolving response proceeds to cytokine activation in the spleen and infarcted LV post-MI

Gene expression analysis for mRNAs encoding 84 inflammatory and adhesion molecules suggested that the leukocyte population in the spleen may coordinate LV repair to resolve post-MI inflammation (Fig. S6 and S7). The mRNAs encoding the pro-inflammatory cytokine IL-1β and the monocyte trafficking marker Ccl2 were consistently higher in the spleen than LV from d1 to d5 post-MI compared to naïve controls. Splenic mRNA levels of *Ccl2* and *IL-1β* were 12.5 and 1200 fold higher than infarcted LV respectively at d5 post-MI (Fig. 8A and 8B). The levels of the mRNA encoding complement component *C3* were decreased within 24 h in both LV and spleen but increased 758 fold at d5 only in the infarcted LV (Fig. 8C), suggestive of complement activation in later stage of post-MI in LV healing. The expression of mRNAs encoding the resolving or reparative cytokines IL-10 (Fig. 8D), CXCL10 (Fig. 8E) and Ccr6 (Fig. 8F) peaked within 24h during the acute inflammatory phase in spleen but took longer to increase in the infarcted LV about d5 post-MI, suggesting that the cytokine response in the infarcted LV was increased during the extended resolving phase at d5 post-MI. These results hint that the innate immune resolving response could be simultaneously activated in the spleen and infarcted LV within 24 h of post-MI. Thus, the resolving response coincides with the acute innate response characterized by increased expression of mRNAs encoding reparative cytokines during LV healing post-MI in mice.

Author Manuscript Author Manuscript Author Manuscript Author Manuscript

Discussion

Innate immune responsive neutrophils ($CD11b^{+}Ly6G^{+}$) and differential macrophages ($CD11b/Ly6C^{high}$ and $CD11b/Ly6C^{low}$) are hallmarks of acute inflammation following myocardial injury. HF individuals show elevated counts of leukocytes in the blood, inflamed arterial wall, and infarcted myocardium post-MI. Post-MI, the spleen provides a steady flow of leukocytes to the infarcted LV. The splenic myelopoiesis coordinates in a time-dependent manner with infarcted LV to determine resolving and non-resolving inflammation in myocardial remodeling (3, 16, 17). Using flow cytometry to identify immune cell populations and LC-MS-MS based metabolomic profiling, we discovered that (i) the spleen may store high levels of PGs (PGD_2 and PGE_2) and SPMs (RvD1, Maresin 1) and macrophages may actively participate in SPM generation during infarcted LV repair (Fig. 8G); (ii) expression of specific LOX-encoding genes were higher in infarcted LV and associated with SPM generation at this site (Fig. 8H); (iii) chemokine response is followed by the cytokine response; and (iv) neutrophils and macrophages not only initiate the acute inflammatory response but may also promote the resolving phase during LV healing. Together, we provide critical knowledge of macrophage-derived SPMs and innate responsive neutrophils and monocyte/macrophages phenotypes that may be therapeutically harnessed without compromising self-defense mechanisms. Additionally, our results rationalize the clinical speculation that splenic metabolic activity predicts the risk of future cardiovascular events (14).

In contrast to the prevailing view that systemic leukocytes and macrophages are the part of pathology leading to inflammatory milieu, we provide evidence that the macrophage secretome of SPMs may be essential for resolving inflammation. Macrophages are present in different organs and generate multiple autocrine and paracrine factors post-MI that are involved in angiogenesis and myocardial healing (18, 19). Diversified subpopulations of macrophages and neutrophils are essential for myocardial healing (15, 18). In addition, our results suggest that macrophages actively produce SPMs in the infarcted LV and spleen to promote resolution of inflammation. Leuschner *et al.* have shown that the post-MI spleen generates monocytes that mobilize to the infarcted LV during acute inflammation. In this process, the local death of neutrophils and monocytes/macrophages is major and the overall cell clearance is minor (16).

Post-MI activated 5LOX not only synthesizes pro-inflammatory LTB_4 to promote recruitment of the leukocytes but also collectively biosynthesizes LXA_4, LXB_4, and AT-LXA_4, which is indicative of a resolution program at the site of myocardium injury. (3, 20). Nuclear translocation of 5LOX is essential to generate pro-inflammatory LTB_4, though RvD1 prevents nuclear translocation of 5LOX, thereby suppressing LTB_4 and enhancing LXA_4 production in macrophages (21). Thus, SPMs (such as RvD1, LXA_4) can orchestrate post-MI cardiac healing mechanisms involving the activation of lipoxin A_4 receptor, thereby reducing mobilization of cytosolic calcium and activation of the calcium-sensitive kinase calcium-calmodulin-dependent protein kinase II (21, 22). Exogenous treatment of RvD1 also activates LXA_4 and MaR1 in murine spleen, suggesting that SPMs act through diversified feed-forward loops to promote resolution without altering acute response post-MI (22). Binary categorization of macrophages and neutrophils into proinflammatory M1 and

Author Manuscript Author Manuscript Author Manuscript Author Manuscript

N1 and proresolving M2 and N2 subsets may be oversimplified but the heterogeneity of M1/M2 or N1/N2 depends on the magnitude of LV injury and paracrine and autocrine role of SPMs (15, 23). The particular leukocyte subset depends on activated COXs and LOXs, availability of omega-3 and −6 fatty acids, and aging, which determine SPM levels in resolving and pro-inflammatory milieu in post-MI healing (24) (Figure 8G–H). Whether the SPMs expand residential macrophage population under the hemodynamic stress of myocardial injury is an area of active research (1, 10, 25).

Comparison of metabololipidomics data from spleen and LV indicated that DHA was enriched in spleen and that it was mobilized to the site of injury with leukocytes post-MI. DHA can extend the life span of lupus prone mice (26). There is general consensus that individuals should maintain balanced intake of n-3 and n-6 fatty acids for optimal health. Dietary supplementation of n-3 fatty acids rich in DHA and EPA has emerged as a preventive strategy to control inflammation in coronary heart disease (27). Imbalances in n-3 and n-6 fatty acids or excessive intake of n-6 fatty acids triggers non-resolving inflammation in aged but not in young mice post-MI (24, 25). The nexus of essential fatty acids and the biosynthesis of the resolution metabolome is an area of active research. Along these lines, Endo *et al.* have created mice that overexpress the *Caenorhabditis elegans* fatty acid desaturase (fat-1) to address discrepancies in dietary studies that can arise from individual genetic and feeding variations. The *fat-1* transgenic mice produce and store higher levels of EPA and DHA in their organs and tissues thereby increasing levels of SPMs. After transverse aortic constriction, *fat-1* transgenic mice show reduced cardiac remodeling with higher levels of EPA metabolites (28).

In summary, the present results provided evidence that post-MI splenic leukocyte infiltration is not only the hallmark of acute inflammatory response but also primes the resolution phase through the production of multiple families of SPMs to activate cardiac resolution program. Future studies with pharmacological restoration of SPMs and on understanding the proresolving role of SPMs are warranted in acute and chronic HF to advance resolution of inflammation in LV tissue regeneration and homeostasis.

Materials and Methods

Animals

Male C57Bl/6J mice (stock number 000664) of 8 to 12 weeks were purchased from The Jackson laboratory, USA. All animal experiments were conducted according to the “Guide for the Care and Use of Laboratory Animals” (8^{th} Edition. 2011), and AVMA Guidelines for the Euthanasia of Animals: (2013 Edition) and were approved by the Institutional Animal Care and Use Committee at the University of Alabama at Birmingham, USA.

Coronary artery ligation to induce myocardial infarction

Mice were anesthetized using continuous isoflurane (2 %) mixed in 100% oxygen through inhalation and then intubated and ventilated with air using a small-animal respirator (Harvard Apparatus, Holliston, MA, USA). The chest hairs were removed using depilatory and a thoracotomy was performed in the fourth left intercostal space. The left atrium and

Author Manuscript Author Manuscript Author Manuscript Author Manuscript

ventricle were observed; the thin pericardium layer was then removed; and the left anterior descending artery was permanently ligated with a 8–0 black polyamide monofilament suture (ARO Surgical, T06A08N14–13) at the site of its emergence (23). Substantial blanching at the LV ischemic area was considered indicative of successful coronary occlusion. The thoracotomy was closed with four 6–0 blue monofilament sutures (Ethicon 6–0 Prolene 8697G). The endotracheal tube was detached once natural respiration resumed, and animals were placed on a warm incubator maintained at 37°C until mice were completely awake (23, 29).

Transthoracic echocardiography

Heart function was measured by echocardiography with a 18–38 MHz transducer using MX-400 Vevo 3100 (VisualSonics Inc., Toronto, Canada) at d0 as naïve control and d1 and d5-post-MI. Mice were sedated with 1–2% isoflurane. Four-limb lead electrocardiograms were simultaneously recorded along with echocardiography. LV fractional shortening (%) was defined as [(EDD-ESD)/EDD] X 100, where EDD is LV end-diastolic dimension and ESD is end-systolic dimension (23, 29).

LV strain and strain rate analysis

LV strain analysis is based on combined speckle tracking algorithms applied on high-frequency ultrasound images. Strain indicates how much the myocardial tissue has deformed: Strain (S) = $\Delta L/L0 = (L1-L0)/L0$. Strain rate reflects how fast the myocardial LV tissue is deforming: Strain rate (SR) = $S/\Delta t = \Delta L/L0/\Delta t$. Thus, strain and strain rate can reflect the global systolic, diastolic and regional LV function. LV strain and strain rate were quantified in the longitudinal, radial, and circumferential axes by speckle tracking of 2D echocardiographic images acquired from the parasternal long- and short-axis views. VevoStrain analyses were conducted by the trained investigator on all animals using VisualSonics software. Short and long axis LV myocardium was automatically divided into six parts for regional speckle tracking. The ultrasound operator was blinded to control and post-MI day samples, which were decoded after strain analyses. (30).

Necropsy procedures for collecting infarcted LV and spleen and infarct area analysis

No-MI naïve controls, post-MI d1 and d5 mice were anesthetized under 2% isoflurane anesthesia in 100% oxygen mix. To collect plasma, mice were injected with heparin (4 IU/g); blood was collected from the carotid artery under isoflurane anesthesia after 5 minutes; and the blood was centrifuged for 5 min to collect plasma. The chest cavity was opened, and the left ventricle was perfused with 2–3 ml cardioplegic solution to remove traces in LV, then the heart, lung and spleen were removed. The lungs and right and left ventricles were collected, weighed and processed as previously described. From the first set of mice, the infarcted LV was collected including the border zone from the apex towards the base. The spleen was dissected by making incision in the left of peritoneal wall. Infarcted LV and spleen (50 mg each) were snap-frozen for targeted metabololipidomic analyses. From the second set of mice, the LV was divided into mid-cavity, apex and base to use the LV mid-cavity for histological analysis and infarcted area for gene expression analyses. The third set of infarcted LV and spleen was used for flow cytometry analyses. LV infarct was

Author Manuscript Author Manuscript Author Manuscript Author Manuscript

confirmed using 2,3,5-triphenyltetrazolium chloride staining at 37°C as described previously (23, 31).

LV and spleen resolution metabololipidomics

LV and spleen samples for LC-MS/MS analysis were extracted using solid phase extraction (SPE) columns as described previously. Briefly, columns were equilibrated with 1 column volume of methanol and 2 volumes ddH2O. Before extraction, 500 pg of deuterium-labeled internal standards d8–5S-HETE, d4LTB_4, d5LXA_4, and d4PGE_2 were added to facilitate quantification of sample recovery. Sample supernatants were diluted with 10 volumes of ddH2O, acidified (pH ~ 3.5) and immediately (< 20–30 seconds) loaded onto the SPE column. After loading, columns were washed with 1 volume of neutral ddH2O followed by hexane. Extracted samples were eluted with 6 ml methyl formate and taken to dryness using Speedvac or nitrogen stream. Samples were suspended in methanol/water for LC-MS/MS. The LC-tandem MS/MS system, QTrap 5500 (ABSciex), was equipped with an Agilent HP1100 binary pump. An Agilent Eclipse Plus C18 column (50 mm x 4.6 mmx 1.8 μm or 100 mm x 4.6 mm x 1.8 μm) was used with a gradient of methanol/water/acetic acid of 60:40:0.01 (volume/volume/volume) to 100:0:0.01 at 0.5-ml/min flow rate. To monitor and quantify the levels of the various LV and spleen lipid mediators, a multiple reaction monitoring method was developed with signature ion fragments for each molecule. Identification was conducted using published criteria with at least 6 diagnostic ions to match the ions in MS-MS spectra and retentions obtained for both authentic and synthetic standards. Calibration curves were obtained using synthetic and authentic LM mixtures (they included d8–5S-HETE, d4-LTB_4, d5-LXA_4, d4-PGE_2, RvD1, RvD2, RvD5, PD1, MaR1, RvE1, RvE2, LXA_4, LXB_4, LXA5, PGE_2, PGD_2, $PGF_{2\alpha}$, thromboxane B2 (TXB_2), PGE_3, $PGF_{3\alpha}$, TXB_3, LTB_4, 17-HDHA, 14-HDHA, 7-HDHA, 4-HDHA, 18-HEPE, 15-HEPE, 12-HEPE, 5-HEPE, 15-HETE, 12-HETE, and 5-HETE) at 12.5, 25, 50, 100 pg. Linear calibration curves for each were obtained with r2 values in the range 0.98–0.99. If a synthetic or biogenic standard for a given product were not available (such as for LXB_5 and PGD_3), calibration curves for products with similar chromatographic behaviors (namely, tri-, di-, or mono-HETEs) to the analyte of interest were used. Quantification was carried out based on the peak area of the MRM transition and the linear calibration curve for each compound (32, 33). All SPMs and prostanoids were identified in accordance with published criteria (32) which included matching retention times, fragmentation patterns, and at least 6 characteristic and diagnostic ions for each as illustrated within the results.

Macrophage depletion

To deplete macrophages, a suspension of clodronate liposomes (Clophosome®; FormuMax Scientific Inc) was prepared for subcutaneous injection (35μg/g body weight) as per the manufacturer's instructions. Briefly, clodronate was injected 24 h (hours) prior to coronary artery ligation and then 3 h post ligation. Post 24 h coronary artery ligation spleen and LV were collected as described above.

Quantitative Real-Time PCR

For qPCR, reverse transcription was performed for both LV and spleen using equal amount of total RNA (2.5μg) using SuperScript® VILO cDNA Synthesis Kit (Invitrogen, CA, USA).

Author Manuscript Author Manuscript Author Manuscript Author Manuscript

Quantitative PCR for *ALOX15* (Mm00507789_m1), *ALOX12* (Mm00545833_m1), *ALOX5* (Mm01182747_m1), *COX-1* (Mm00477214_m1) and *COX-2* (Mm00478374_m1) genes was performed using taqman probes (Applied Biosystems, CA, USA) on master cycler ABI, 7900HT. Gene expression was normalized to the housekeeping control gene *Hprt-1* (Mm01545399_m1) (which encodes hypoxanthine phosphoribosyltransferase). The results were reported as $2^{-\Delta Ct}$ ($\Delta\Delta Ct$) values. All the experiments were performed in duplicates with n=4 mice/group/day.

Flow cytometry

Single mononuclear cells were isolated from d0 naïve controls and at post-MI d1 and d5. Infarcted LV and spleen of male C57Bl/6J mice were analyzed by flow cytometry (24). Prior to isolation, LV was perfused as described above to remove blood traces. The cell count for LV mononuclear cells or splenocytes were adjusted to ~1–2 million cells/stain. Isolated cell suspensions were finally suspended in 200μl of 1:500Fc block and incubated for 10 min on ice. A cocktail of fluorophore-labeled monoclonal antibodies in 2X concentration were added for 30 min on ice as appropriate for each set. We used CD45-PE (BD Biosciences), CD11b-APC, F4/80-Percp (molecular probes), Ly6C-FITC (BD Biosciences), Ly6G-pacific blue (e-bioscience) and CD206-PE (Biolegend) in cocktail. All populations were first gated using $CD45^+$ as a marker for hematopoietic cells. Further, the neutrophils were defined as $CD11b^+/Ly6G^+$ cells. Activated macrophages were defined as cells with dual expression of CD11b (Mac-1) and the surface marker $F4/80^+$. The macrophages ($F4/80^+$) were also classified as M1 (classically activated macrophages) or M2 (alternatively activated macrophages) based on $Ly6C^{high}/CD206^-$ and $Ly6C^{low}/CD206^+$ respectively. Similarly, neutrophils were defined as N1 ($Ly6G^+/CD206^-$) and N2 ($Ly6G^+/CD206^+$). Data were acquired on BDTM LSRII Flow Cytometer and analyzed with FlowJo software, version 7.6.3. The gating strategy is shown in Fig S8.

LV and spleen inflammatory array

To understand the kinetics of inflammatory response and to reach target specific approach post-MI, simultaneously in LV and spleen we did 84 gene-expression arrays. Frozen samples for d0 control and post-MI d1 or d5 from infarcted LV (LVI) and spleen were processed separately for RNA extraction. LVI and spleen tissue (4–8 mg) was homogenized with a sonic dismembrator (Fisher Scientific Inc. USA, amplitude between 10–100) and RNA was isolated using TRIzol (Invitrogen) as per the manufacturer's instructions. RNA concentrations were determined using the ND1000 Nano drop. cDNA synthesis was performed RT2 first strand kit (Qiagen 330401) using 400ng RNA per sample. LV sample gene expression was prepared using RT^2-profiler PCR array [Inflammatory Cytokine and Receptor by Qiagen (PAMM-011E)] and run on an ABI 7900HT. Gene expression levels were normalized to the housekeeping control gene *Hprt-1*. The results were reported as normalized expression values (23, 31).

Statistical analysis

Data are expressed as mean±SEM. One-way ANOVA post-hoc Kruskal-Wallis was used to compare measures with ≥2 independent groups. Comparisons between groups (no-MI control, d1 and d5 post-MI) were performed with Dunn multiple-comparisons test when the

Author Manuscript Author Manuscript Author Manuscript Author Manuscript

ANOVA test was statistically significant. The Mann–Whitney test was used to compare 2 groups. A value of $p<0.05$ was considered significant.

Supplementary Material

Refer to Web version on PubMed Central for supplementary material.

Acknowledgments:

We thank Iliyan Vlasakov of the Center for Experimental Therapeutics and Reperfusion Injury for expert technical assistance in sample preparation for LC-MS-MS.

Funding: This work was supported by National Institutes of Health [AT006704 and HL132989] and The University of Alabama at Birmingham (UAB) Pittman scholar award to G.V.H., American Heart Association postdoctoral fellowship [POST31000008] to V.K. and [P01-GM095467 and GM038765–30] to C.N.S.

References and Notes

1. Kain V, Prabhu SD, Halade GV, Inflammation revisited: inflammation versus resolution of inflammation following myocardial infarction. Basic Res Cardiol 109, 444 (2014). [PubMed: 25248433]
2. Prabhu SD, Frangogiannis NG, The Biological Basis for Cardiac Repair After Myocardial Infarction: From Inflammation to Fibrosis. Circ Res 119, 91–112 (2016). [PubMed: 27340270]
3. Tourki B, Halade G, Leukocyte diversity in resolving and nonresolving mechanisms of cardiac remodeling. FASEB J 31, 4226–4239 (2017). [PubMed: 28642328]
4. Serhan CN, Yacoubian S, Yang R, Anti-inflammatory and proresolving lipid mediators. Annual review of pathology 3, 279–312 (2008).
5. Tabas I, Glass CK, Anti-inflammatory therapy in chronic disease: challenges and opportunities. Science 339, 166–172 (2013). [PubMed: 23307734]
6. Frangogiannis NG, Regulation of the inflammatory response in cardiac repair. Circ Res 110, 159–173 (2012). [PubMed: 22223212]
7. Nahrendorf M, Frantz S, Swirski FK, Mulder WJ, Randolph G, Ertl G, Ntziachristos V, Piek JJ, Stroes ES, Schwaiger M, Mann DL, Fayad ZA, Imaging Systemic Inflammatory Networks in Ischemic Heart Disease. J Am Coll Cardiol 65, 1583–1591 (2015). [PubMed: 25881940]
8. Bolli R, Reflections on the Irreproducibility of Scientific Papers. Circ Res 117, 665–666 (2015). [PubMed: 26405183]
9. Swirski FK, Nahrendorf M, Etzrodt M, Wildgruber M, Cortez-Retamozo V, Panizzi P, Figueiredo JL, Kohler RH, Chudnovskiy A, Waterman P, Aikawa E, Mempel TR, Libby P, Weissleder R, Pittet MJ, Identification of splenic reservoir monocytes and their deployment to inflammatory sites. Science 325, 612–616 (2009). [PubMed: 19644120]
10. Serhan CN, Pro-resolving lipid mediators are leads for resolution physiology. Nature 510, 92–101 (2014). [PubMed: 24899309]
11. Funk CD, Leukotriene modifiers as potential therapeutics for cardiovascular disease. Nat Rev Drug Discov 4, 664–672 (2005). [PubMed: 16041318]
12. Antman EM, Bennett JS, Daugherty A, Furberg C, Roberts H, Taubert KA, Use of nonsteroidal antiinflammatory drugs: an update for clinicians: a scientific statement from the American Heart Association. Circulation 115, 1634–1642 (2007). [PubMed: 17325246]
13. Dutta P, Courties G, Wei Y, Leuschner F, Gorbatov R, Robbins CS, Iwamoto Y, Thompson B, Carlson AL, Heidt T, Majmudar MD, Lasitschka F, Etzrodt M, Waterman P, Waring MT, Chicoine AT, van der Laan AM, Niessen HW, Piek JJ, Rubin BB, Butany J, Stone JR, Katus HA, Murphy SA, Morrow DA, Sabatine MS, Vinegoni C, Moskowitz MA, Pittet MJ, Libby P, Lin CP, Swirski FK, Weissleder R, Nahrendorf M, Myocardial infarction accelerates atherosclerosis. Nature 487, 325–329 (2012). [PubMed: 22763456]

Author Manuscript Author Manuscript Author Manuscript Author Manuscript

14. Emami H, Singh P, MacNabb M, Vucic E, Lavender Z, Rudd JH, Fayad ZA, Lehrer-Graiwer J, Korsgren M, Figueroa AL, Fredrickson J, Rubin B, Hoffmann U, Truong QA, Min JK, Baruch A, Nasir K, Nahrendorf M, Tawakol A, Splenic metabolic activity predicts risk of future cardiovascular events: demonstration of a cardiosplenic axis in humans. JACC Cardiovasc Imaging 8, 121–130 (2015). [PubMed: 25577441]
15. Ma Y, Yabluchanskiy A, Iyer RP, Cannon PL, Flynn ER, Jung M, Henry J, Cates CA, Deleon-Pennell KY, Lindsey ML, Temporal neutrophil polarization following myocardial infarction. Cardiovasc Res 110, 51–61 (2016). [PubMed: 26825554]
16. Leuschner F, Rauch PJ, Ueno T, Gorbatov R, Marinelli B, Lee WW, Dutta P, Wei Y, Robbins C, Iwamoto Y, Sena B, Chudnovskiy A, Panizzi P, Keliher E, Higgins JM, Libby P, Moskowitz MA, Pittet MJ, Swirski FK, Weissleder R, Nahrendorf M, Rapid monocyte kinetics in acute myocardial infarction are sustained by extramedullary monocytopoiesis. The Journal of experimental medicine 209, 123–137 (2012). [PubMed: 22213805]
17. Ismahil MA, Hamid T, Bansal SS, Patel B, Kingery JR, Prabhu SD, Remodeling of the mononuclear phagocyte network underlies chronic inflammation and disease progression in heart failure: critical importance of the cardiosplenic axis. Circ Res 114, 266–282 (2014). [PubMed: 24186967]
18. Aurora AB, Porrello ER, Tan W, Mahmoud AI, Hill JA, Bassel-Duby R, Sadek HA, Olson EN, Macrophages are required for neonatal heart regeneration. J Clin Invest 124, 1382–1392 (2014). [PubMed: 24569380]
19. Libby P, Nahrendorf M, Swirski FK, Leukocytes Link Local and Systemic Inflammation in Ischemic Cardiovascular Disease: An Expanded “Cardiovascular Continuum”. J Am Coll Cardiol 67, 1091–1103 (2016). [PubMed: 26940931]
20. Blomer N, Pachel C, Hofmann U, Nordbeck P, Bauer W, Mathes D, Frey A, Bayer B, Vogel B, Ertl G, Bauersachs J, Frantz S, 5-Lipoxygenase facilitates healing after myocardial infarction. Basic Res Cardiol 108, 367 (2013). [PubMed: 23812248]
21. Fredman G, Ozcan L, Spolitu S, Hellmann J, Spite M, Backs J, Tabas I, Resolvin D1 limits 5-lipoxygenase nuclear localization and leukotriene B4 synthesis by inhibiting a calcium-activated kinase pathway. Proc Natl Acad Sci U S A, (2014).
22. Kain V, Ingle KA, Colas RA, Dalli J, Prabhu SD, Serhan CN, Joshi M, Halade GV, Resolvin D1 activates the inflammation resolving response at splenic and ventricular site following myocardial infarction leading to improved ventricular function. J Mol Cell Cardiol 84, 24–35 (2015). [PubMed: 25870158]
23. Ma Y, Halade GV, Zhang J, Ramirez TA, Levin D, Voorhees A, Jin YF, Han HC, Manicone AM, Lindsey ML, Matrix metalloproteinase-28 deletion exacerbates cardiac dysfunction and rupture after myocardial infarction in mice by inhibiting M2 macrophage activation. Circ Res 112, 675–688 (2013). [PubMed: 23261783]
24. Halade GV, Kain V, Black LM, Prabhu SD, Ingle KA, Aging dysregulates D- and E-series resolvins to modulate cardiosplenic and cardiorenal network following myocardial infarction. Aging (Albany NY) 8, 2611–2634 (2016). [PubMed: 27777380]
25. Lopez EF, Kabarowski JH, Ingle KA, Kain V, Barnes S, Crossman DK, Lindsey ML, Halade GV, Obesity superimposed on aging magnifies inflammation and delays the resolving response after myocardial infarction. Am J Physiol Heart Circ Physiol 308, H269–280 (2015). [PubMed: 25485899]
26. Halade GV, Rahman MM, Bhattacharya A, Barnes JL, Chandrasekar B, Fernandes G, Docosahexaenoic acid-enriched fish oil attenuates kidney disease and prolongs median and maximal life span of autoimmune lupus-prone mice. Journal of immunology 184, 5280–5286 (2010).
27. Mozaffarian D, Wu JH, Omega-3 fatty acids and cardiovascular disease: effects on risk factors, molecular pathways, and clinical events. J Am Coll Cardiol 58, 2047–2067 (2011). [PubMed: 22051327]
28. Endo J, Sano M, Isobe Y, Fukuda K, Kang JX, Arai H, Arita M, 18-HEPE, an n-3 fatty acid metabolite released by macrophages, prevents pressure overload-induced maladaptive cardiac remodeling. J Exp Med 211, 1673–1687 (2014). [PubMed: 25049337]

Author Manuscript Author Manuscript Author Manuscript Author Manuscript

29. Halade GV, Kain V, Ingle KA, Heart Functional and Structural Compendium of Cardiosplenic and Cardiorenal Networks in Acute and Chronic Heart Failure Pathology. Am J Physiol Heart Circ Physiol, ajpheart 00528 02017 (2017).

30. Bauer M, Cheng S, Jain M, Ngoy S, Theodoropoulos C, Trujillo A, Lin FC, Liao R, Echocardiographic speckle-tracking based strain imaging for rapid cardiovascular phenotyping in mice. Circ Res 108, 908–916 (2011). [PubMed: 21372284]

31. Halade GV, Ma Y, Ramirez TA, Zhang J, Dai Q, Hensler JG, Lopez EF, Ghasemi O, Jin YF, Lindsey ML, Reduced BDNF attenuates inflammation and angiogenesis to improve survival and cardiac function following myocardial infarction in mice. Am J Physiol Heart Circ Physiol 305, H1830–1842 (2013). [PubMed: 24142413]

32. Dalli J, Serhan CN, Specific lipid mediator signatures of human phagocytes: microparticles stimulate macrophage efferocytosis and pro-resolving mediators. Blood 120, e60–72 (2012). [PubMed: 22904297]

33. Colas RA, Shinohara M, Dalli J, Chiang N, Serhan CN, Identification and signature profiles for pro-resolving and inflammatory lipid mediators in human tissue. Am J Physiol Cell Physiol 307, C39–54 (2014). [PubMed: 24696140]

Author Manuscript Author Manuscript Author Manuscript Author Manuscript

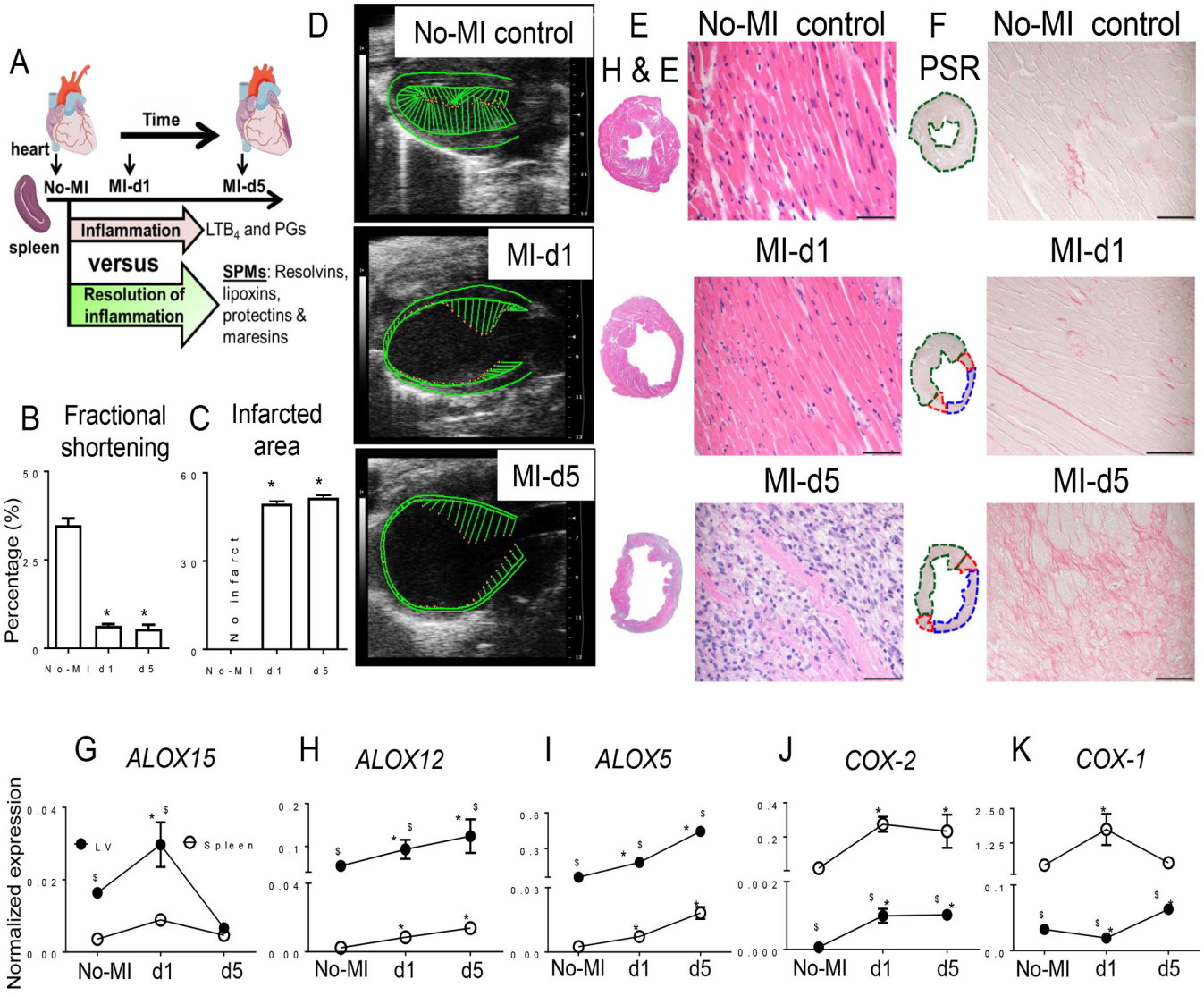


Figure 1. Infarcted LV healing is associated with expression of different *LOX* isoforms in mice post-MI.

A. Study design. B. Fractional shortening (%) measured from the long axis. n=6 mice/group/day. C. Post-MI percentage of LV infarcted area compared to naïve controls with no infarct. n=6 mice/group/day. D. Representative echocardiographic long axis B-mode images of naïve control, and post-MI d1 and d5. E and F. Representative images from horizontal sections of LV mid-cavity stained with (E) hematoxylin and eosin and (F) picrosirius red. Scale bar, 50 μm. n=6 mice/group/day. G to I. Expression analysis of (G) *ALOX15*, (H) *ALOX12*, (I) and *ALOX5* in infarcted LV or spleen from naïve control mice or at the indicated time points after MI. Expression was normalized to Hprt-1. n=6 mice/group/day. J-K. Expression analysis of (J) *COX-2* and (K) *COX-1* in infarcted LV from naïve control mice or at the indicated time points post-MI. *LOX* and *COX* gene expression was normalized to *Hprt-1*. N=6 mice/group/day. *p<0.05 compared to no-MI naïve control and $p<0.05 compared to spleen at respective day time point using one way ANOVA.

Author Manuscript Author Manuscript Author Manuscript Author Manuscript

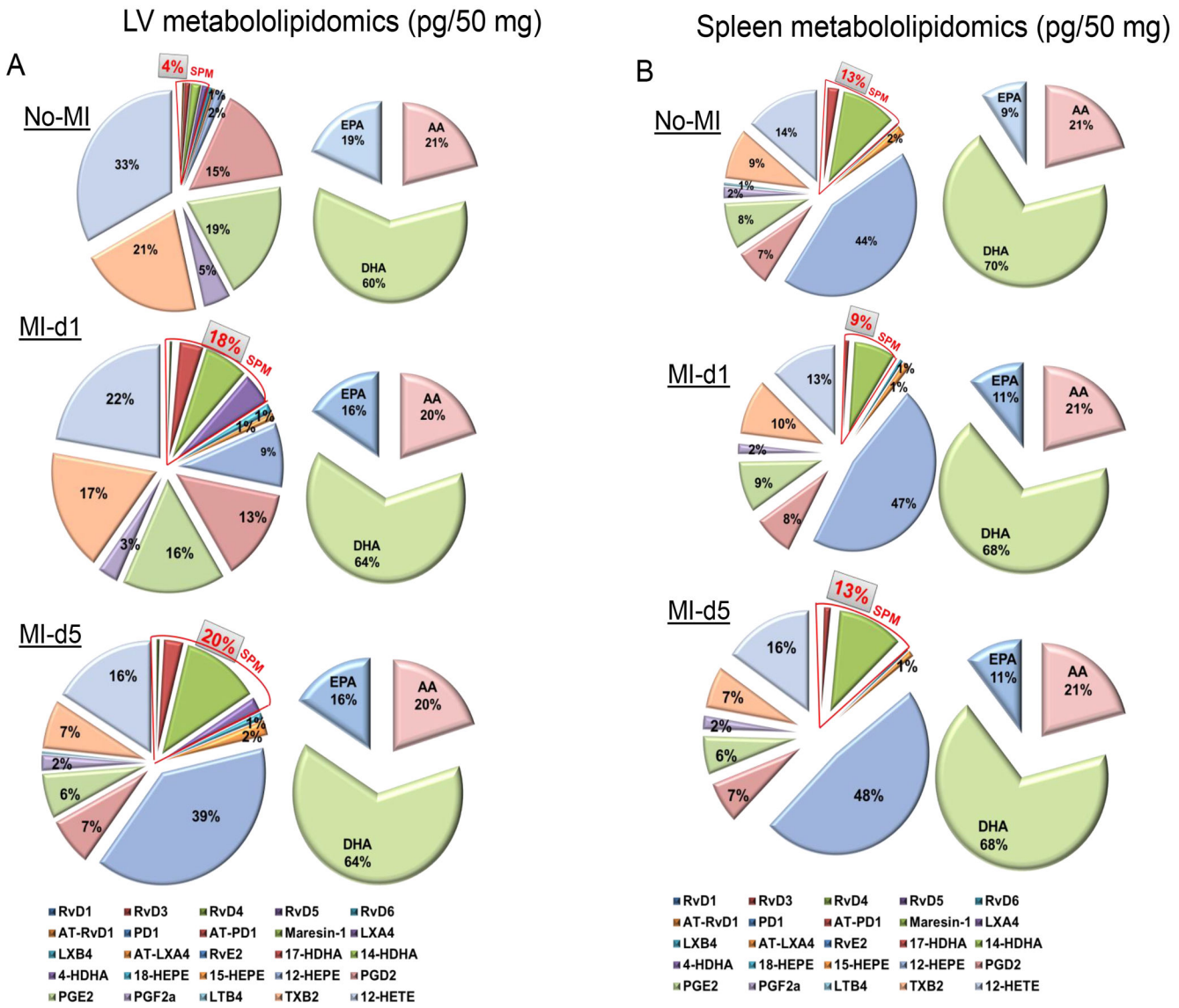


Figure 2. SPM biosynthesis peaked in the infarcted LV and was reduced in spleen post-MI within 24 h.

A. Pie chart representing the distribution of SPMs and docosahexaenoic acid (DHA), eicosapentaenoic acid (EPA) and arachidonic acid (AA) in infarcted LV from naïve control mice or at the indicated time points post-MI. n=4 mice/group/day. B. Pie chart representing the distribution of SPMs and docosahexaenoic acid (DHA), eicosapentaenoic acid (EPA) and arachidonic acid (AA) metabolome in spleen from naïve control mice or at the indicated time points post-MI. Percentage of mean values for each of the lipid mediators identified are presented in the pie chart. n=4 mice/group/day. Quantification and values are pg/ 50 mg LV tissue from apex to base and pg/50mg spleen tissue. The detection limit was ~1 pg.

Author Manuscript Author Manuscript Author Manuscript Author Manuscript

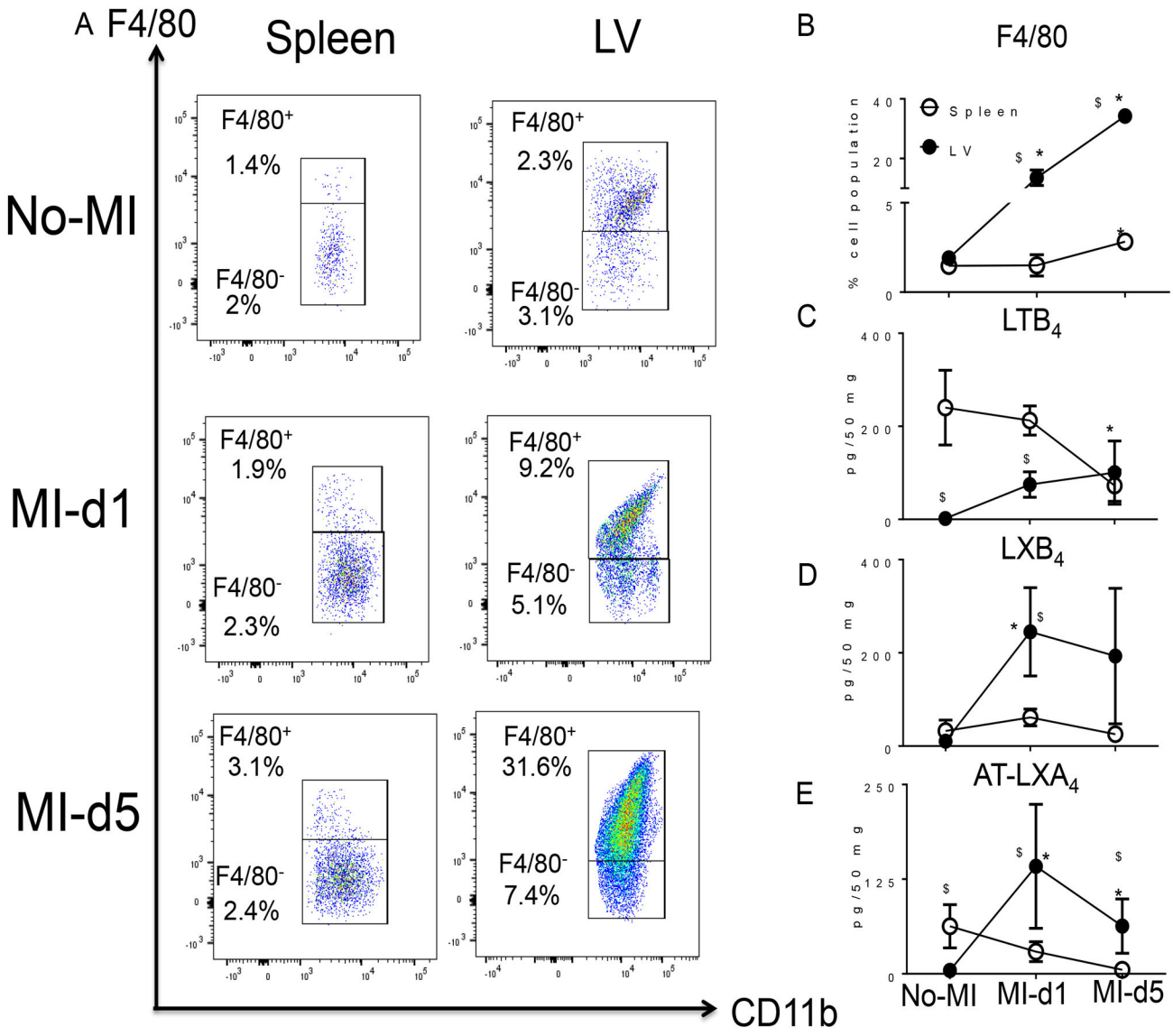


Figure 3. Infarcted LV macrophage activation is inversely proportional to lipoxin kinetics in the spleen within 24 h post-MI.

A. Representative flow cytometry (FACs) dot plots showing the macrophage population ($CD11b^+/F4/80^+$) in spleen (left panel) and LV mononuclear cells (right panel) in no-MI naïve control and at d1 and d5 post-MI. B. Line graph showing the percentage of the $F4/80^+$ population in spleen and LV mononuclear cells at d0, post-MI d1 and d5. n=4 mice/group/day. C. Line graph showing the kinetics of LTB_4 in LV and spleen in no-MI control and at d1 and d5 post-MI. n=4 mice/group/day. D. Line graph showing the kinetics of LXB_4 in no-MI control and at d1 and d5 post-MI in LV and spleen. n=4 mice/group/day. E. Line graph showing the kinetics of AT-LXA_4 in LV and spleen in no-MI control and at d1 and d5 post-MI. Results are mean±SEM. Quantification and values in C, D, and E are pg/50 mg of spleen or infarcted LV tissue from apex to base. The detection limit was ~1 pg. *$p<0.05$ compared to no-MI naïve control and \$$p<0.05$ compared to spleen at respective day time point using one way ANOVA.

Author Manuscript
Author Manuscript
Author Manuscript
Author Manuscript

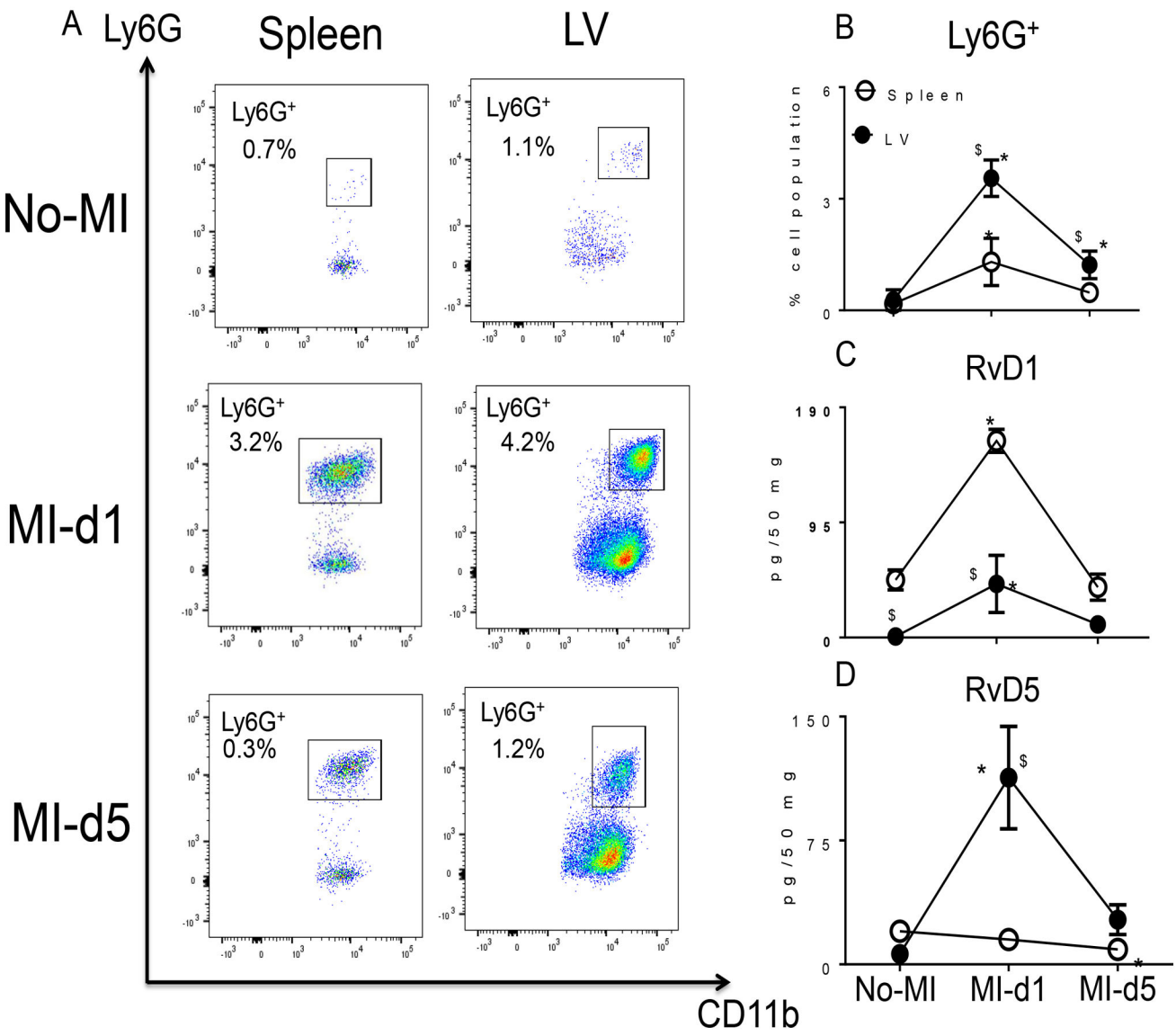


Figure 4. Infarcted LV contains activated leukocytes and SPM biosynthesis is increased in spleen and infarcted myocardium post-MI.

A. Representative flow cytometry (FACs) dot plots showing the neutrophil population ($CD11b^+/Ly6G^+$) in spleen (left panel) and LV mononuclear cells (right panel) in no-MI naïve control and at d1 and d5 post-MI. B. Line graph showing the percentage of the $Ly6G^+$ population in spleen and LV mononuclear cells at d0, and d1 and d5 post-MI. n=4 mice/group/day. C. Line graph showing the kinetics of RvD1 in LV and spleen in no-MI control and at d1 and d5 post-MI. n=4 mice/group/day. D. Line graph showing the kinetics of RvD5 in LV and spleen at d1 and d5 post-MI compared to spleen and LV d0 naïve controls. n=4 mice/group/day. Quantification and values in C and D are pg/50 mg of spleen or infarcted LV tissue from apex to base. *$p<0.05$ compared to no-MI naïve control and \$$p<0.05$ compared to spleen at respective day time point using one way ANOVA.

Author Manuscript Author Manuscript Author Manuscript Author Manuscript

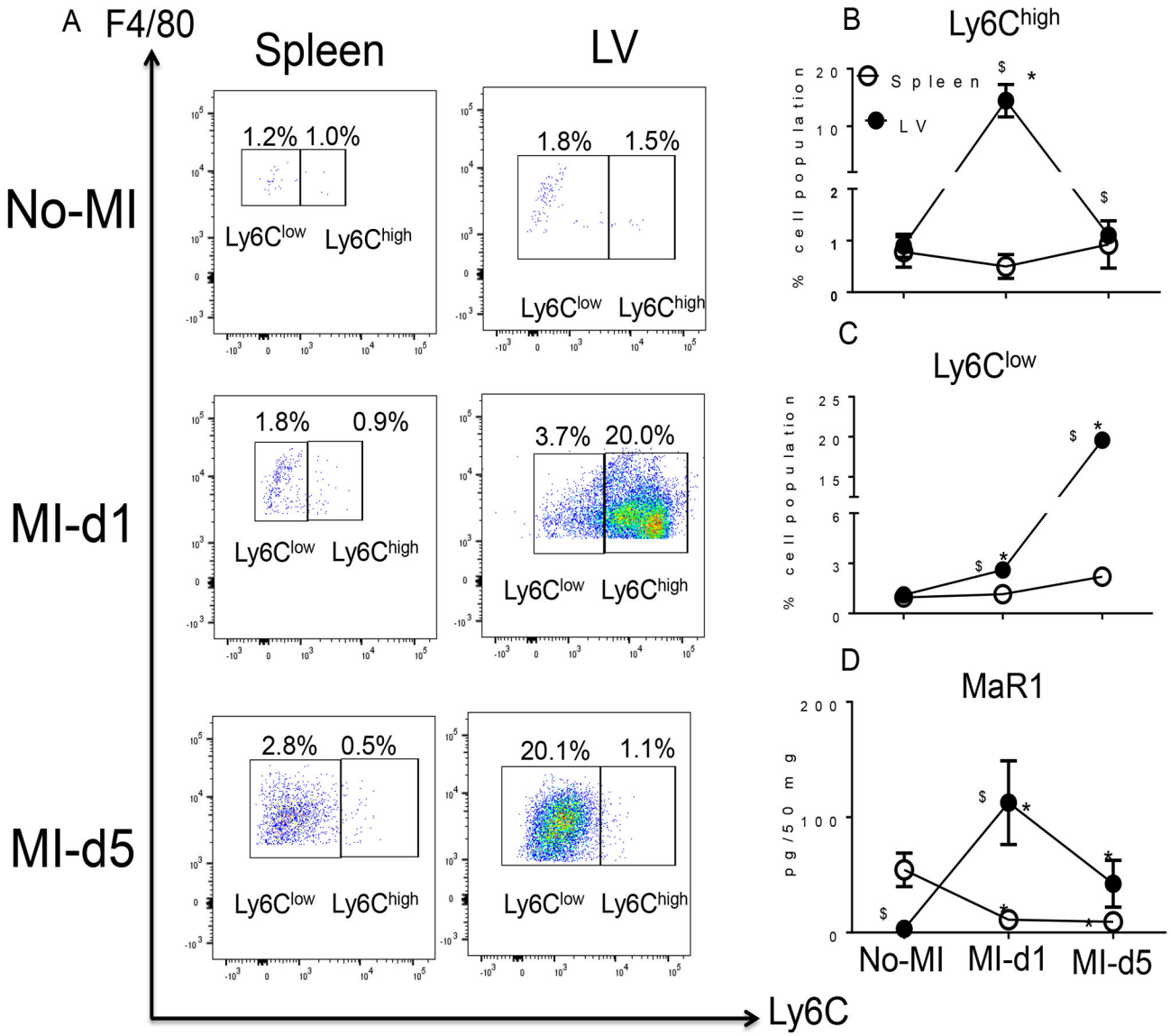


Figure 5. Splenic monocyte/macrophage subsets (F4/80^{+}/Ly6Cl^{ow}) that increase in the infarcted LV within 24 h are associated with biosynthesis of maresin 1 (MaR1).

A. Representative flow cytometry (FACs) dot plots showing macrophage population (F4/80^{+}/Ly6C^{+}) in spleen (left panel) and LV mononuclear cells (right panel) in no-MI naive control and at d1 and d5 post-MI. B. Line graph showing the percentage of the Ly6C^{high} population in spleen and LV mononuclear cells at d0, d1 and d5 post-MI. n=4 mice/group/day. C. Line graph showing the percentage of the Ly6C^{low} population in spleen and LV mononuclear cells in d0 naïve controls and at d1 and d5 post-MI. n=4 mice/group/day. D. Line graph showing the kinetics of MaR1 in LV and spleen in no-MI control and at d1 and d5 post-MI. n=4 mice/group/day. Results are mean±SEM. Quantification and values of analytes are pg/50 mg of spleen or LV infarct tissue from apex to base. The detection limit was ~1 pg. *p<0.05 compared to no-MI naïve control. $p<0.05 compared to spleen at respective day time point using one way ANOVA.

Author Manuscript Author Manuscript Author Manuscript Author Manuscript

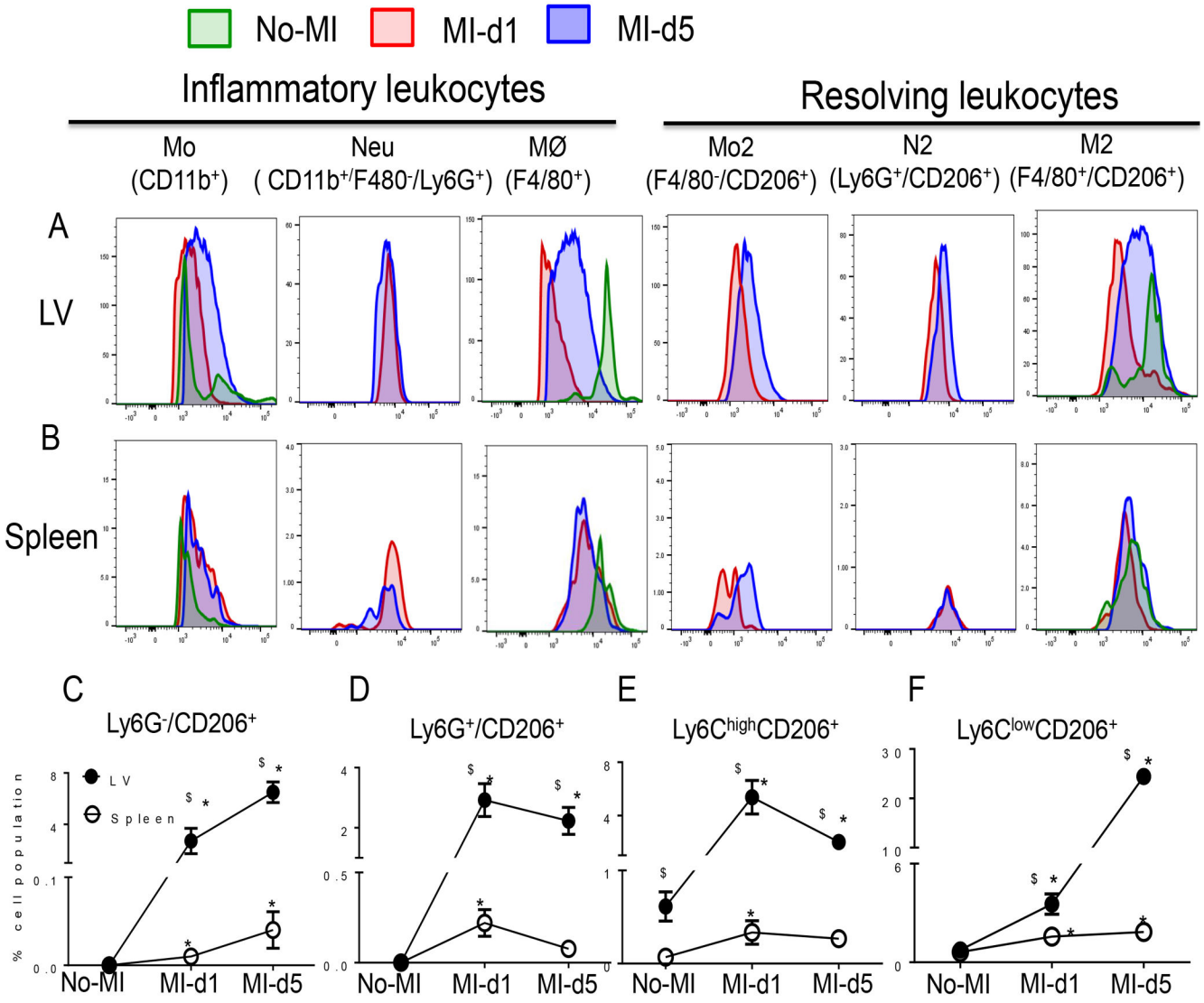


Figure 6. Leukocyte activation in infarcted LV and spleen is associated with overlapping inflammatory and resolving phenotypes.

A. Representative histogram overlay of inflammatory and resolving leukocytes in LV. n=4 mice/group/day. B. Representative histogram overlay of inflammatory and resolving leukocytes in spleen. n=4 mice/group/day. C-F. Line graphs showing the kinetics of the C. $Ly6G^{-}/CD206^{+}$ D. $Ly6G^{+}/CD206^{+}$ E. $Ly6C^{high}/CD206^{+}$ F. and $Ly6C^{low}/CD206^{+}$ populations in LV and spleen. Results are expressed as mean±SEM, n=4 mice/group/day. *p<0.05 compared to no-MI naïve control and $p<0.05 compared to spleen at respective day time point using one way ANOVA (Mo; monocytes, Neu; Neutrophils, MØ; macrophages; N2 resolving neutrophils, M2; resolving macrophages)

Author Manuscript Author Manuscript Author Manuscript Author Manuscript

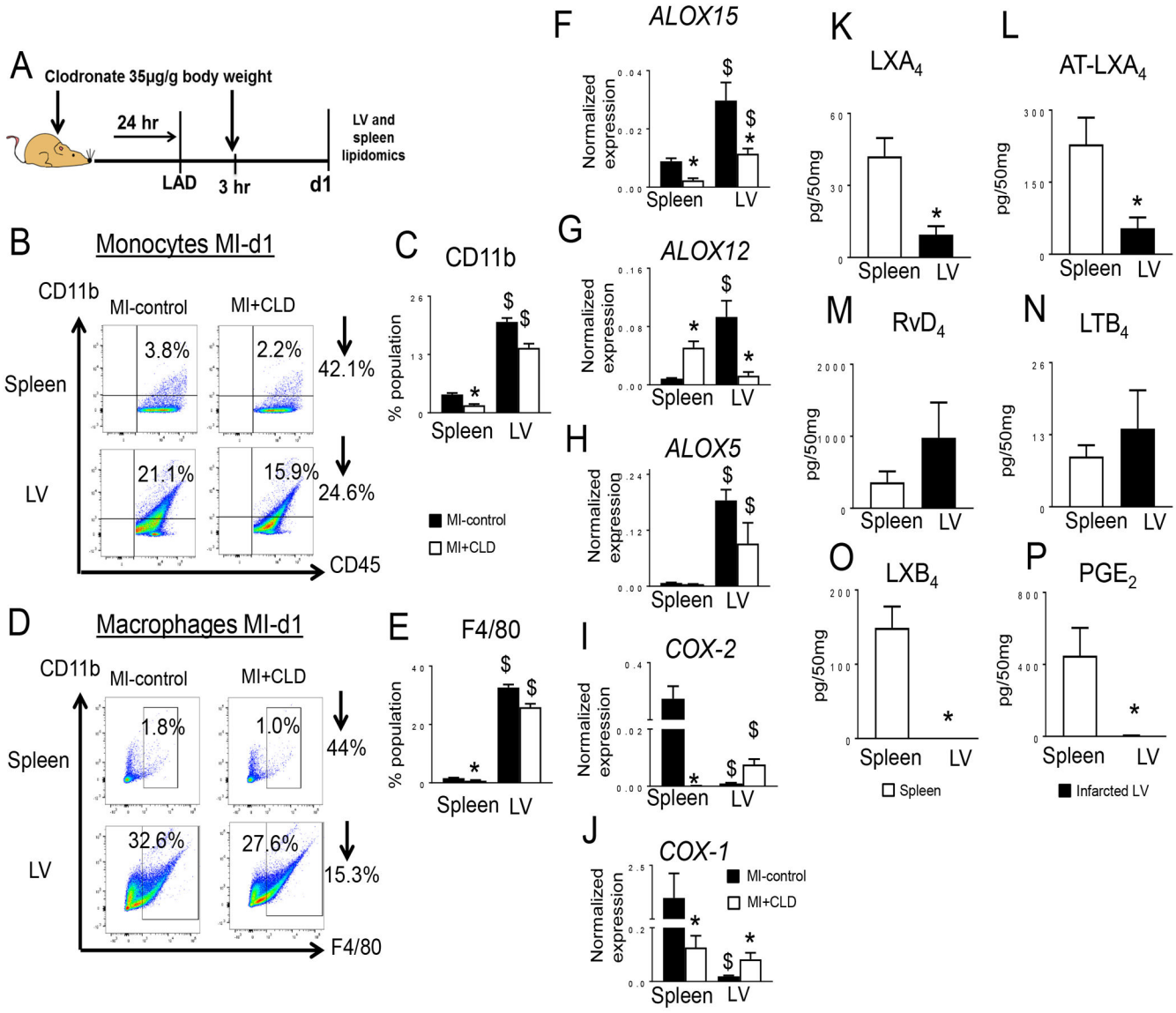


Figure 7. Macrophage depletion reduced LOXs expression thereby SPMs post-MI.

A. Scheme illustrating the experimental design for clodronate (CLD) treatment in MI model. B. Representative flow cytometry (FACs) dot plots showing the monocyte population ($CD11b^+CD45^+$) mononuclear cells in spleen (upper panel) and infarcted LV (lower panel) in MI-control and CLD injected mice. C. Bar graph representing $CD11b^+$ cells. D. FACs dot plots showing the mononuclear macrophage population ($CD11b^+F4/80^+$) in spleen (upper panel) and infarcted LV (lower panel) in MI-control and CLD-injected mice. E. Bar graph representing $F4/80^+$ cells (open bar MI-control and filled bar MI+CLD). n=4 mice/group. F-H. Gene expression analysis of F. *ALOX15,* G. *ALOX12,* H *ALOX5,* in infarcted LV post-MI in CLD-injected mice. Gene expression was normalized to *Hprt-1.* n=4 mice/group. I-J. Gene expression analysis of I. *COX-2*, J. *COX-1* in infarcted LV post-MI in CLD-injected mice. Gene expression was normalized to *Hprt-1.* n=4 mice/group. *p<0.05 compared to MI control and $p<0.05 compared to spleen using one way ANOVA. K-P. Measurement of K.

Author Manuscript Author Manuscript Author Manuscript Author Manuscript

LXA_4, L. AT-LXA_4, M. RvD4, N. LTB_4, O. LXB_4, and P. PGE_2 in spleen (open bar) and infarcted LV (filled bar) at day 1 post-MI after CLD-mediated macrophage depletion. Results are Mean±SEM values; n=3 mice/group. Quantified values of analytes are pg/50 mg of spleen or LV infarct tissue from apex to base. The detection limit was ~1 pg.

Author Manuscript
Author Manuscript
Author Manuscript
Author Manuscript

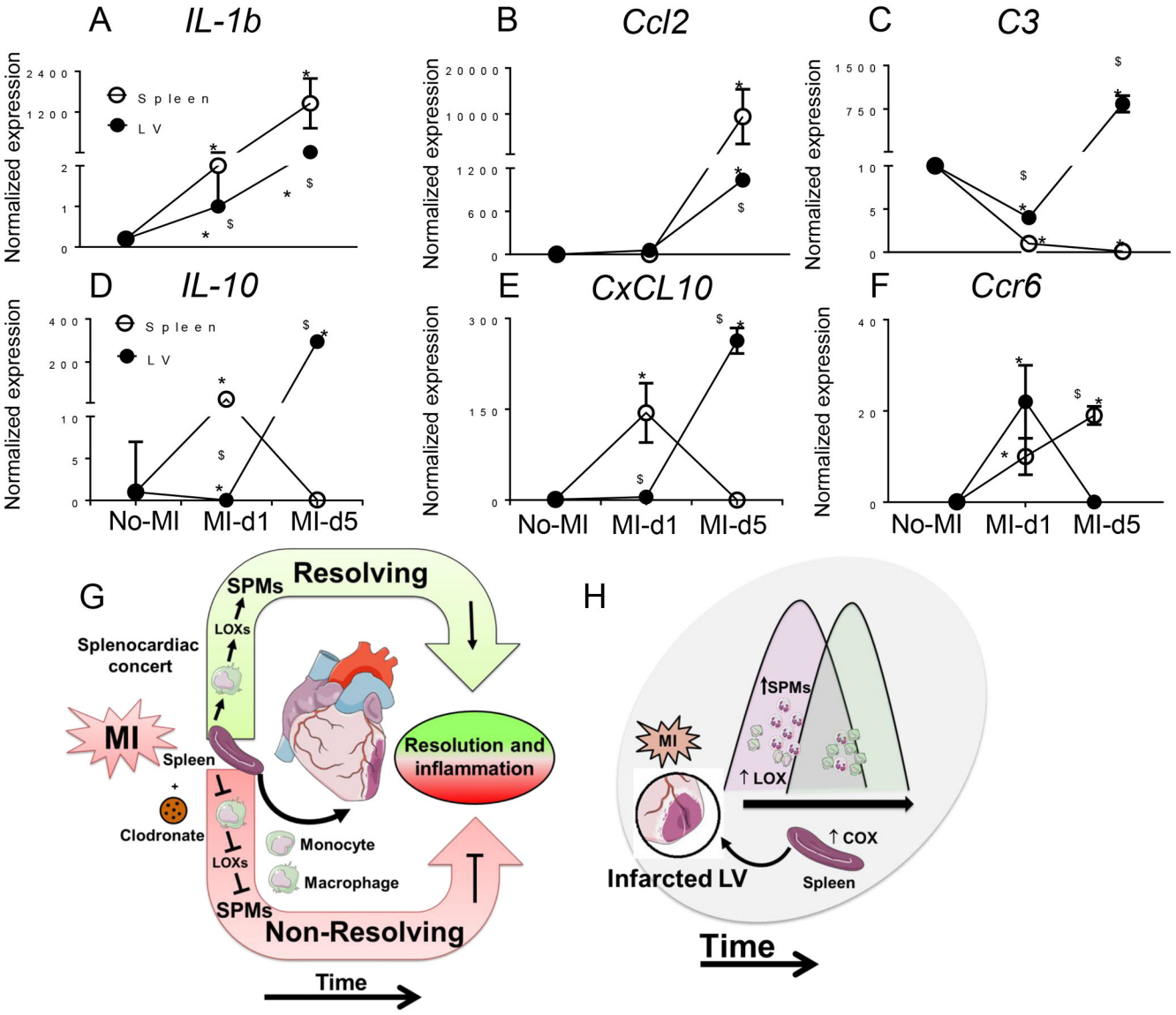


Figure 8. Activated cytokine and chemokine signal is amplified early in spleen than LV in post-MI resolution of inflammation.

A-F. mRNA expression of A. *IL-1b*, B. *Ccl2*, C *C3,* D. *IL-10,* E. *CxCL10*, and F. *Ccr6* in spleen or infarcted LV from naïve control mice or at the indicated time points post-MI. Results are expressed as mean±SEM, n=4 mice/group. *p<0.05 compared to no-MI naïve control and $p<0.05 compared to spleen at respective day time point using one way ANOVA. G. Model showing that leukocytes in the spleen generated SPMs through LOX isoforms that advance the resolution of inflammation and healing in the LV post-MI. Clodronate (CLD)-mediated macrophage depletion reduced the expression of *LOX* isoforms and generation of SPMs, thereby triggering non-resolving inflammation that can lead to HF. H. Model showing that post-MI, LOXs are preferentially activated in the infarcted LV to generate SPMs that promote cardiac repair.

Author Manuscript

Author Manuscript

Author Manuscript

Author Manuscript

Table 1.

MI-induced edema in LV is marked with splenic mass depletion.

Parameters	No-MI (naïve controls)	MI day 1	MI day 5
Mice (n)	10	10	10
Body weight (g)	22.4 ± 1.0	24.3 ± 1.6	21.9 ± 0.6
LV weight (mg)	72.1 ± 2.0	85.4 ± 5.3*	100.6 ± 2.4*
Spleen weight (mg)	62.5 ± 3.2	53.4 ± 4.9*	80.8 ± 5.3*
LV/tibia	4.3 ± 0.1	5.1 ± 0.3*	6.1 ± 0.1*
Lung weight (mg)	154 ± 19	142 ± 13	184 ± 22*

LV; left ventricle, MI; myocardial infarction,

*P<0.05 compared to no-MI naïve controls by ANOVA